

BCS-BEC crossover on the two-dimensional honeycomb lattice

Erhai Zhao¹ and Arun Paramekanti¹

¹*Department of Physics, University of Toronto, Toronto, Ontario M5S-1A7, Canada*

The attractive Hubbard model on the honeycomb lattice exhibits, at half-filling, a quantum critical point (QCP) between a semimetal with massless Dirac fermions and an s-wave superconductor (SC). We study the BCS-BEC crossover in this model away from half-filling at zero temperature and show that the appropriately defined crossover line (in the interaction-density plane) passes through the QCP at half-filling. For a range of densities around half-filling, the “underlying Fermi surface” of the SC, defined as the momentum space locus of minimum energy quasiparticle excitations, encloses an area which changes nonmonotonically with interaction. We also study fluctuations in the SC and the semimetal, and show the emergence of an undamped Leggett mode deep in the SC. Finally, we consider possible implications for ultracold atoms in optical lattices and the high temperature SCs.

PACS numbers: 03.75.Kk, 03.75.Ss, 74.20.-z

The close connection between the Bardeen-Cooper-Schrieffer (BCS) theory of superconductivity and the phenomenon of Bose-Einstein condensation (BEC) is clearly revealed by studies of the BCS-BEC crossover problem [1]. One can experimentally access this crossover in harmonically trapped atomic gases by tuning the s-wave atom-atom scattering length a_s using a magnetic field induced Feshbach resonance [2, 3, 4, 5, 6, 7]. The low temperature phase of these atomic gases crosses over from a BCS state for $a_s < 0$ to a molecular BEC for $a_s > 0$. Experiments [8, 9] and theory [10, 11, 12] have also begun to address the issue of strongly interacting fermionic atoms in optical lattices. The ETH measurements [8] of the population distribution in different bands upon tuning through a Feshbach resonance were explained partially by focussing on a *single* well in the lattice [10]. In addition, it was conjectured that this system could show a band insulator to SC transition with increasing interaction [10] at low temperature; however multiband effects [10] complicate a microscopic analysis of this problem.

Motivated by exploring a simpler model which displays such a transition and can be realized using cold atoms, we study the attractive Hubbard model,

$$H = - \sum_{i,j,\sigma} t_{ij} c_{i\sigma}^\dagger c_{j,\sigma} - U \sum_i n_{i\uparrow} n_{i\downarrow} - \mu \sum_{i,\sigma} n_{i\sigma}, \quad (1)$$

on a two-dimensional (2D) honeycomb lattice, with hopping amplitude $t_{ij} = t$ to nearest-neighbor sites and $t_{ij} = t'$ to next-nearest neighbors (see Fig.1). Noninteracting fermions ($U = 0$) at half-filling (one fermion per site on average) on this lattice form a semimetal, with the “Fermi surface” shrunk to Fermi points. This semimetal behaves like a band insulator in some respects, displaying a vanishing density of states at zero energy and two bands (a “conduction” and a “valence” band) which touch at two inequivalent Fermi points, $\pm\mathbf{K}$, in momentum space as shown in Fig.1 (the two bands arise from having two sites per unit cell on the honeycomb lattice). We show that turning on interactions in this model leads

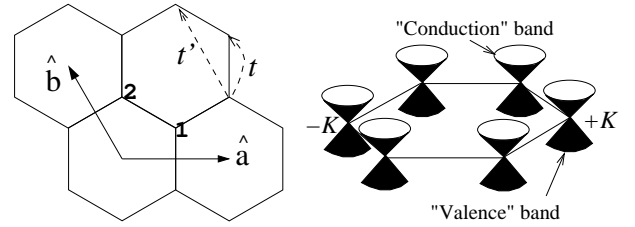


FIG. 1: Left: Honeycomb lattice showing basis vectors and the two sites per unit cell, as well as the hopping matrix elements in model (1). Right: Quasiparticle dispersion with Dirac nodes in first Brillouin zone of the noninteracting semimetal.

to rich physics associated with a semimetal-SC transition at half-filling and a BCS-BEC crossover away from half-filling when U becomes comparable to the kinetic energy $\sim t$. Bands other than those in model (1) can, however, be ignored so long as they are separated by interband gaps $\gg U, t$.

Compared to earlier studies of the BCS-BEC crossover [13], our following results are unusual. (i) The conventional BCS-BEC crossover is unrelated to any quantum phase transition (QPT), describing the smooth evolution from a weakly paired to a strongly paired SC state. By contrast, model (1) at half-filling exhibits a QPT between a semimetal and a SC at a critical interaction, $U = U_c$. (ii) Away from half-filling, it displays a BCS-BEC crossover. As shown in Fig.2(a), the appropriately defined BCS-BEC crossover line in the interaction-density plane passes through the quantum critical point (QCP) at half-filling, suggesting that the finite temperature normal state near the crossover could be strongly influenced by this QCP, especially for small density deviations from half-filling (“small doping”). (iii) For small dopings, the “underlying Fermi surface” (UFS) of the SC [14, 15], defined as the momentum space locus of minimum energy quasiparticle excitations, exhibits nonmonotonic behavior with increasing U in contrast to its monotonically shrinking area in the continuum [14]. (iv) The fluctuations in the SC phase of model (1) are like those

of a two-band SC [16] and support an undamped Leggett mode [17] deep in the BEC regime (Fig.3(a)). (v) In contrast to a Fermi liquid, long wavelength SC fluctuations in the semimetal have a damping proportional to energy (Fig.3(b)) due to the Dirac fermions. We discuss the relevance of some of these results the high temperature SCs in the concluding section.

Model and mean-field theory: We write the partition function of model (1) as $\mathcal{Z} = \int \mathcal{D}\psi \exp(-S)$, with $S = \int_0^\beta d\tau \left\{ \sum_{\alpha,\beta,\mathbf{k}} \bar{\psi}_{\alpha\mathbf{k}\sigma}(\tau) [\delta_{\alpha\beta} \partial_\tau + h_{\alpha\beta}(\mathbf{k})] \psi_{\beta\mathbf{k}\sigma}(\tau) - U \sum_{i,\alpha} \bar{\psi}_{\alpha,i,\uparrow}(\tau) \bar{\psi}_{\alpha,i,\downarrow}(\tau) \psi_{\alpha,i,\downarrow}(\tau) \psi_{\alpha,i,\uparrow}(\tau) \right\}$ where i refers to a site on the triangular lattice, and $\alpha = 1, 2$ labels the two sites within the unit cell (sublattice index). The matrix elements $h_{\alpha\beta}(\mathbf{k})$ are given by $h_{11}(\mathbf{k}) = h_{22}(\mathbf{k}) = x_{\mathbf{k}}$, and $h_{21}(\mathbf{k}) = h_{12}^*(\mathbf{k}) = \gamma_{\mathbf{k}}$ with $x_{\mathbf{k}} = -2t'(\cos \mathbf{k} \cdot \hat{a} + \cos \mathbf{k} \cdot \hat{b} + \cos \mathbf{k} \cdot \hat{c}) - \mu$ and $\gamma_{\mathbf{k}} = -t(1 + e^{i\mathbf{k} \cdot \hat{b}} + e^{-i\mathbf{k} \cdot \hat{a}})$. Here \hat{a}, \hat{b} are unit vectors shown in Fig.1, and $\hat{c} = \hat{a} + \hat{b}$. We introduce [16, 18] Hubbard-Stratonovich fields $\Delta_{\alpha,i}(\tau)$ to decouple the interaction term in the pair channel. The mean-field theory (MFT) of the SC is obtained by setting $\Delta_{\alpha,i}(\tau) \equiv \Delta_0$, integrating out the fermions, and extremizing the action with respect to Δ_0 . This leads to the gap equation

$$\frac{1}{U} = \frac{1}{N} \sum_{\nu=\pm,\mathbf{k}} \frac{1}{2E_{\mathbf{k}}^\nu} \tanh\left(\frac{\beta E_{\mathbf{k}}^\nu}{2}\right). \quad (2)$$

Here ν labels the two bands [19], $E_{\mathbf{k}}^\pm = \sqrt{\xi_\pm^2(\mathbf{k}) + \Delta_0^2}$ is the excitation energy of Bogoliubov quasiparticles in MFT with $\xi_\pm(\mathbf{k}) = x_{\mathbf{k}} \pm |\gamma_{\mathbf{k}}|$, and N is the number of sites on the honeycomb lattice. Using $\partial \mathcal{F}_{\text{MF}} / \partial \mu = -N_e$, the fermion density $n = N_e / N$ is

$$n = 1 - \frac{1}{N} \sum_{\nu=\pm,\mathbf{k}} \frac{\xi_\nu(\mathbf{k})}{E_{\mathbf{k}}^\nu} \tanh\left(\frac{\beta E_{\mathbf{k}}^\nu}{2}\right). \quad (3)$$

Figs.2(a,b) show the MF values of Δ_0, μ obtained by numerically solving (2) and (3) over a range of densities and interaction strengths.

At half-filling ($n = 1$) and for $t' < t/3$, the noninteracting ($U = 0$) ground state is a semimetal with $\Delta_0 = 0$ and $\mu = 3t'$. The single-particle spectrum consists of massless Dirac fermions, centered around $\mathbf{K} \equiv (\pm 4\pi/3, 0)$ and dispersing at low energy as $\xi_\pm(\mathbf{k}) \sim \pm v_F |\mathbf{k} - \mathbf{K}|$, with a Fermi velocity $v_F = t\sqrt{3}/2$. This leads to a linearly vanishing density of states (DOS) of single-particle excitations at low energy, $N(\omega) = \frac{\sqrt{3}}{4\pi v_F} \omega$ per spin, which renders the semimetal *stable* to weak attractive interactions in contrast to a Fermi liquid. At large enough interactions $U > U_c$, the semimetal becomes unstable to an ordered state, similar to that in a model studied by Nozieres and Pistoiesi [20]. For $t' = 0$, both SC and charge density wave solutions are degenerate due to a special SU(2) symmetry. This degeneracy is lifted at nonzero t' , and

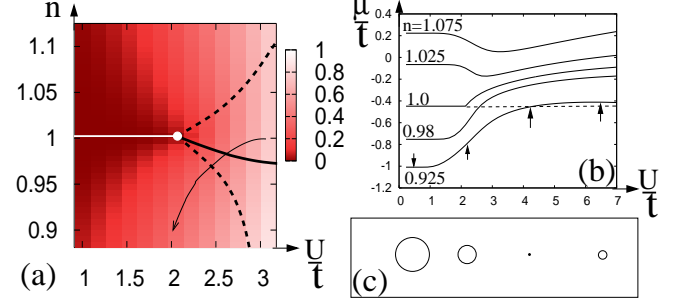


FIG. 2: (a) (Color online) Plot of the mean field gap, Δ_0/t , versus n and U/t (for $t' = -0.15t$). White horizontal line at $n = 1$ is the semimetal phase terminating in a semimetal-SC transition at $U_c/t \approx 2.13$. Dashed lines indicate the BCS-BEC crossover discussed in the text. Thick black line indicates the parameters at which the “underlying Fermi surface” (UFS), discussed in text and panels (b) and (c), shrinks to a point. The light arrow indicates a possible trajectory of the Hamiltonian discussed in the text. (b) Mean field chemical potential μ/t versus U/t for indicated fillings ($t' = -0.15t$). Dashed line at $\mu = 3t'$ is a guide to the eye. (c) Schematic “underlying Fermi surface” (see text), roughly circular loci around the nodes $\pm \mathbf{K}$, drawn for parameters indicated by arrows in panel (b).

we find that the SC state has lower energy justifying our Hubbard-Stratonovich decoupling in the pairing channel. The mean field gap $\Delta_0 \sim (U - U_c)$ for U close to U_c while for large U , $\Delta_0 \simeq U/2$. We fix $t' = -0.15t$, where $U_c \approx 2.13t$, and focus here only on the SC order and its fluctuations. (For $t' = 0$, MF, variational, and Monte Carlo numerics yield estimates $U_c \sim 2t - 5t$ [21].)

Away from half-filling, with a doping $\delta n \equiv n - 1$, the noninteracting ground state has small Fermi pockets centered around $\pm \mathbf{K}$, and is unstable to SC for an arbitrarily small U . The DOS scales as $\sqrt{|\delta n|}/v_F$ leading to $\Delta_0 \sim \sqrt{|\delta n|} \exp[-gv_F/(U \sqrt{|\delta n|})]$ for $U \ll v_F \sqrt{|\delta n|}$ (with $g^2 = 16\pi/\sqrt{3}$), where $v_F \sqrt{|\delta n|}$ acts like an effective Fermi energy. This weak coupling SC evolves into a BEC regime at larger U .

(i) *BCS-BEC crossover:* A mean field estimate of the crossover to the BEC regime is obtained by requiring that the SC gap $\Delta_0(U, \delta n)$ be larger than either (i) the Fermi energy of the doped carriers in the noninteracting limit $\mu(U = 0, \delta n) - 3t'$ or (ii) the chemical potential $\mu(U, n) - 3t'$, where $3t' \equiv \mu(U = 0, \delta n = 0)$. Fig.2(a) shows this crossover line plotted using criterion (i); however both definitions yield the qualitatively similar result that the BCS-BEC crossover line (defined away from half-filling) passes through the QCP (at half-filling). If the Hamiltonian describing the doped system lies on a trajectory such as shown in Fig.2(a), with a density-dependent U , then the system will undergo a BEC-BCS crossover for parameters which lie close to the QCP; the finite temperature normal state near the crossover is then expected to be strongly influenced by this QCP.

(ii) *Underlying Fermi surface*: We define the “underlying Fermi surface” (UFS) of the SC as the locus of points around $\pm\mathbf{K}$ where the quasiparticle excitation gap is a minimum [14]. At weak coupling, this UFS is identical to the FS of the doped metallic phase, which is approximately a circle centered around $\pm\mathbf{K}$. Turning on interactions at small doping leads to a strong change in μ . In fact, for a range of doping $\delta n < 0$ (for $t' < 0$), μ goes from the “valence” into the “conduction” band leading to the evolution of the UFS as shown in Fig.2(c). Eventually, at a large enough gap, the UFS begins to decrease [22] as in the continuum case [14]. The UFS is thus not related in any way to the Fermi surface of the underlying noninteracting metal [14, 15]. For example, at a certain interaction value for low doping we find $\mu = 3t'$; since the chemical potential then sits at the node of the Dirac dispersion it leads to a point-like UFS as seen in Fig.2(c). For this value of U , the *strongly interacting doped* SC would appear, if naively viewed as a weak coupling SC, to have descended from an *undoped* semimetal.

Superfluid density, Estimate of T_c : Going beyond MFT, we expand $\Delta_{\alpha\mathbf{q}}(\tau) = \Delta_0 + \Lambda_{\alpha\mathbf{q}}(\tau)$ around its mean field value and integrate out the fermions to arrive at the effective action for order parameter fluctuations, $S_{\text{RPA}} = \sum_q \hat{\Lambda}_q^\dagger \hat{W}_q \hat{\Lambda}_q$, to second order in $\Lambda_{\alpha,q}$. Here $q \equiv (\mathbf{q}, i\omega_n)$, and $\hat{\Lambda}_q = (\Lambda_{1,q}, \Lambda_{1,-q}^*, \Lambda_{2,q}, \Lambda_{2,-q}^*)^T$ defines the vector of order parameter fluctuations on the 1, 2 sublattices. We further separate the fluctuation into its amplitude (real) and phase (imaginary) components [18] $\Lambda_{\alpha,q} = \Delta_0[r_{\alpha,q} + i\varphi_{\alpha,q}]$, and integrate out the (gapped) amplitude fluctuations to obtain the effective 2×2 matrix action for phase fluctuations

$$S[\varphi] = \frac{\beta}{2} \sum_q (\varphi_{1,q}^*, \varphi_{2,q}^*) \begin{pmatrix} u_q & v_q \\ v_q^* & u_q \end{pmatrix} \begin{pmatrix} \varphi_{1,q} \\ \varphi_{2,q} \end{pmatrix} \quad (4)$$

Diagonalizing this leads to two eigenmodes, the Goldstone mode φ_G and the Leggett mode φ_L , with $S[\varphi] = (\beta/2) \sum_q [(u_q - |v_q|)|\varphi_{G,q}|^2 + (u_q + |v_q|)|\varphi_{L,q}|^2]$. The zero temperature superfluid density, $D_s(0)$, is obtained by examining the Goldstone mode action in the limit $\omega = 0$. In this static limit, amplitude and phase fluctuations decouple, and $u_q \rightarrow u_{\mathbf{q}}, v_q \rightarrow v_{\mathbf{q}}$ simplify to

$$u_{\mathbf{q}} = \frac{2\Delta_0^2}{U} - \frac{\Delta_0^2}{2N} \sum_{\mathbf{k},\nu,\sigma} \frac{\cos^2(\theta_{\mathbf{k}}^\nu - \theta_{\mathbf{k}-\mathbf{q}}^\sigma)}{E_{\mathbf{k}}^\nu + E_{\mathbf{k}-\mathbf{q}}^\sigma}, \quad (5)$$

$$v_{\mathbf{q}} = -\frac{\Delta_0^2}{2N} \sum_{\mathbf{k},\nu,\sigma} \nu\sigma \frac{\cos^2(\theta_{\mathbf{k}}^\nu - \theta_{\mathbf{k}-\mathbf{q}}^\sigma)}{E_{\mathbf{k}}^\nu + E_{\mathbf{k}-\mathbf{q}}^\sigma} \frac{\gamma_{\mathbf{k}}^* \gamma_{\mathbf{k}-\mathbf{q}}}{|\gamma_{\mathbf{k}}| |\gamma_{\mathbf{k}-\mathbf{q}}|} \quad (6)$$

where $\nu, \sigma = \pm$, and $\theta_{\mathbf{k}}^\nu$ are defined by $\sin 2\theta_{\mathbf{k}}^\nu = \Delta/E_{\mathbf{k}}^\nu$ and $\cos 2\theta_{\mathbf{k}}^\nu = -\xi_\nu(\mathbf{k})/E_{\mathbf{k}}^\nu$. We numerically extract the zero temperature superfluid stiffness, $D_s(0)$, by identifying $u_{\mathbf{q}} - |v_{\mathbf{q}}| \equiv (\sqrt{3}D_s(0)/2)\mathbf{q}^2$ for $|\mathbf{q}| \rightarrow 0$.

The SC-normal transition temperature at weak coupling is mainly determined by the vanishing of Δ_0 due to

thermally excited quasiparticles. The mean field transition temperature T_c^0 , where $\Delta_0 \rightarrow 0$, is obtained by generalizing and solving the mean field gap and number equations at nonzero temperature [22]. At strong coupling, T_c is governed by the superfluid stiffness. We estimate the Kosterlitz-Thouless (KT) transition temperature as $T_{\text{KT}}^* = \pi D_s(0)/2$. The SC transition temperature is then approximately given by $T_c = \min(T_c^0, T_{\text{KT}}^*)$. Fig.3(a) displays the crossover region between the BCS ($T_c \sim T_c^0$) and BEC ($T_c \sim T_{\text{KT}}^*$) regimes. We also find that the highest transition temperature $T_c^{\text{max}} \sim 0.1t$.

Leggett mode, Goldstone mode: In order to study collective modes in the SC, we retain time-dependent fluctuations around the MFT, which couples amplitude and phase fluctuations leading to a 4×4 fluctuation matrix. Examination of the four eigenmodes reveals that one mode is gapless and corresponds to a linearly dispersing Goldstone mode. The remaining three modes are gapped: two of these correspond to amplitude fluctuations while the third mode corresponds to a Leggett mode [17] (relative fluctuations of φ within a unit cell) of this “two-band” superfluid [16]. Integrating out the amplitude modes, leads to complicated expressions for u_q, v_q which will be presented in detail elsewhere [22]. Using these, we have numerically evaluated the Goldstone mode velocity, c_G [22], as well as the gap to the Leggett mode, ω_L , as a function of U and n . At weak coupling, the Leggett mode at $\mathbf{q} = 0$ has weight only at energies above $2\Delta_0$ and is strongly damped by the two-quasiparticle continuum in the SC. With increasing U , however, it emerges undamped (below the continuum) in the regime indicated in Fig.3(a). $\omega_L/2\Delta_0$ decreases monotonically with increasing U in this regime. The Leggett mode can be excited by making small oscillations in opposite directions of the optical lattice potential on the two sublattices [22].

Fluctuations in the semi-metal: The Gaussian action in the semimetal can be derived by studying fluctuations around $\Delta_0 = 0$. We again separate the fluctuations into real and imaginary parts (these no longer have the meaning of ‘amplitude’ and ‘phase’ fluctuations) and obtain the propagator $\langle r_{\alpha,q}^* r_{\alpha,q} \rangle = \langle \varphi_{\alpha,q}^* \varphi_{\alpha,q} \rangle$ from the fluctuation matrix [22]. In Fig.3(b), the spectral function $A(\mathbf{q}, \omega) = \text{Im}\langle r_{\alpha,q}^* r_{\alpha,q} \rangle$ is plotted for various values of \mathbf{q} at $U = 2.1t$. The lineshape of $A(\mathbf{q}, \omega)$ can be understood by analyzing the DOS of the decay channel for SC fluctuations in the semimetal, viz. two-particle excitations with total momentum \mathbf{q} . At $\mathbf{q} = 0$, this is proportional to the single particle DOS in the semimetal and increases linearly with energy. For small but nonzero \mathbf{q} there is a threshold $v_F|\mathbf{q}|$ above which damping onsets. For large momenta, the threshold again vanishes at the wavevector connecting the Dirac nodes. Thus, the long wavelength SC fluctuations, which have a gap E_g that vanishes as $U \rightarrow U_c$, are critically damped (i.e., have damping \sim energy) if $|\mathbf{q}| < E_g/v_F$. For larger \mathbf{q} the mode begins

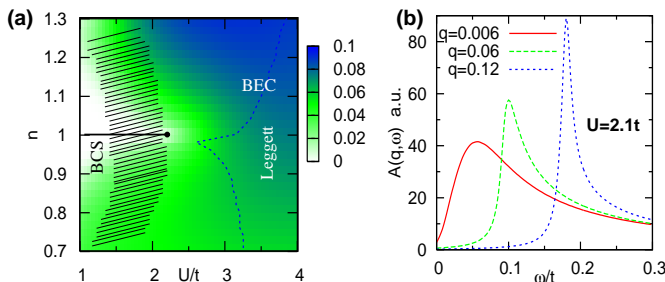


FIG. 3: (Color online) **(a)** Plot of the SC transition temperature, $T_c = \min(T_c^0, T_{KT}^*)$ (see text). Shaded region is the crossover regime between $T_c \sim T_c^0$ (“BCS”) and $T_c \sim T_{KT}^*$ (“BEC”). Region marked “Leggett”, beyond the dashed line, indicates parameters where an undamped Leggett mode emerges. Solid horizontal line at $n = 1$ is the semimetal terminating at a QCP. **(b)** Spectral function (in arbitrary units) of SC fluctuations in the semimetal at $U = 2.1t$. Small \mathbf{q} fluctuations appear critically damped, with the damping threshold being strongly \mathbf{q} -dependent. Large \mathbf{q} fluctuations can propagate as undamped modes when close to the QCP.

to emerge from the two-particle continuum and sharpens (see Fig.3(b)). For large enough \mathbf{q} it can propagate as an undamped mode for U sufficiently close to U_c .

Discussion: The honeycomb lattice attractive Hubbard model exhibits a quantum phase transition between a semimetal and a SC, and a BCS-BEC crossover at low doping which lies near the transition. This model could be studied experimentally using two-component fermionic atoms in a honeycomb lattice potential which can be generated using three blue-detuned laser beams [23]. Our work is also of broad relevance to the high temperature cuprate SCs. The cuprate SCs have a d-wave order parameter and descend from a Mott insulating antiferromagnet [24]. Nevertheless, studies of the BCS-BEC crossover problem in lattice *s-wave* SCs [1, 18] clarified the physics of SCs with a large pairing gap and a small superfluid density, and were relevant to the understanding aspects of the pseudogap regime. There are similar connections between our model and the cuprates. (a) Superconductivity in the cuprates is widely viewed as resulting from doping a spin liquid insulator [24] — a model relevant to the undoped spin liquid is the staggered flux phase [25] which, in mean field theory, has nodal Dirac fermions similar to our undoped semimetal. (b) The SC crosses over with increasing doping from a strongly correlated (BEC-like) to a weakly correlated (BCS-like) state [1], with the normal state above T_c at optimal doping displaying proximity to an as-yet-unknown QCP. (c) Recent photoemission experiments in underdoped cuprates appear to find an anomalous metallic phase with a point-like FS as the normal state of underdoped cuprates [26]. Our results on the crossovers in a SC state close to a semimetal-SC QCP, and the evolution of the UFS in the crossover regime could shed light on observations (b),(c) in the cuprates. Given these connections, and also the

viability of realizing this model with ultracold atoms in an optical lattice, it would be interesting to explore its phase diagram in experiments.

Acknowledgments: We thank G. Baskaran, A. Griffin, M. Randeria, E. Taylor, A. Vishwanath and especially H. Moritz for discussion and comments. This work was supported by NSERC and a Connaught startup grant.

-
- [1] For reviews, see: M. Randeria, in *Bose-Einstein Condensation*, edited by A. Griffin, D. Snoke and S. Stringari (Cambridge University Press, 1994); V. M. Loktev, *et al*, Phys. Rep. **349**, 1 (2001); Q. Chen, *et al*, Phys. Rep. **412**, 1 (2005).
 - [2] C. A. Regal, *et al*, Phys. Rev. Lett. **92**, 040403 (2004).
 - [3] M. W. Zwierlein *et al.*, Phys. Rev. Lett. **92**, 120403 (2004).
 - [4] J. Kinast *et al.*, Phys. Rev. Lett. **92**, 150402 (2004).
 - [5] M. Bartenstein *et al.*, Phys. Rev. Lett. **92**, 120401 (2004); **92**, 203201 (2004).
 - [6] T. Bourdel *et al.*, Phys. Rev. Lett. **93**, 050401 (2004).
 - [7] G. B. Partridge *et al.*, Phys. Rev. Lett. **95**, 020404 (2005).
 - [8] M. Köhl, *et al*, Phys. Rev. Lett. **94**, 080403 (2005).
 - [9] J. K. Chin, *et al*, cond-mat/0607004 (unpublished).
 - [10] R. B. Diener and T.-L. Ho, Phys. Rev. Lett. **96**, 010402 (2006).
 - [11] L.-M. Duan, Phys. Rev. Lett. **95**, 243202 (2005).
 - [12] A. O. Koetsier, *et al*, cond-mat/0604186.
 - [13] L. Belkhir and M. Randeria, Phys. Rev. B **45**, 5087 (1992); N. Trivedi and M. Randeria, Phys. Rev. Lett. **75**, 312 (1995); N. Dupuis, Phys. Rev. B **70**, 134502 (2004); T. Paiva, *et al*, Phys. Rev. B **69**, 184501 (2004).
 - [14] R. Sensarma, *et al*, cond-mat/0607006 (unpublished).
 - [15] C. Gros, *et al*, cond-mat/0606750 (unpublished).
 - [16] M. Iskin and C. A. R. Sa de Melo, Phys. Rev. B **72**, 024512 (2005); S.G. Sharapov, *et al*, Eur. Phys. J. B **30**, 45 (2002).
 - [17] A. J. Leggett, Progr. Theor. Phys. **36**, 901 (1966).
 - [18] M. Randeria, *et al*, Phys. Rev. B **41**, 327 (1990); J. R. Engelbrecht, *et al*, Phys. Rev. B **55**, 15153 (1997).
 - [19] For $t' \neq 0$, the \pm bands are not in one-to-one correspondence with the “valence”/“conduction” bands.
 - [20] P. Nozieres and F. Pistolesi, Eur. Phys. J. B **10**, 469 (1999).
 - [21] At $t' = 0$, a particle-hole transformation leads to a repulsive Hubbard model, which has been numerically studied by: S. Sorella and E. Tosatti, Europhys. Lett. **19**, 699 (1992); N. Furukawa, J. Phys. Soc. Jpn. **70**, 1483 (2001); L. M. Martelo, *et al*, Z. Phys. B: Condens. Matter **103**, 335 (1997); T. Paiva *et al.*, Phys. Rev. B **72**, 085123 (2005).
 - [22] E. Zhao and A. Paramekanti, in preparation.
 - [23] L.-M. Duan, E. Demler and M.D. Lukin, Phys. Rev. Lett. **91**, 090402 (2003).
 - [24] P. A. Lee, N. Nagaosa, and X.-G. Wen, Rev. Mod. Phys. **78**, 17 (2006).
 - [25] J. B. Marston and I. Affleck, Phys. Rev. B **39**, 11538 (1989).
 - [26] A. Kanigel, *et al*, Nature Physics **2**, 447 (2006).